A new methodology for assessing SAR despeckling filters

Rubén Darío Vásquez-Salazar[1], Ahmed Alejandro Cardona-Mesa[2], Luis Gómez[3], *Senior Member, IEEE*, and Carlos M. Travieso-Gonzalez[4]

***Abstract*—Supervised learning requires labeled data to train models and then make predictions from new input data. Deep Learning (DL) methods require immense amounts of training data and processing power to provide reasonable results. In computer vision applications, and more specifically in despeckling SAR (Synthetic Aperture Radar) images, due to the speckle content, there is no ground truth available. To test the performances of despeckling filters, the common approach is to corrupt synthetic images with a suitable speckle model and then, after filtering, well-known metrics are obtained. Then, filters are tested on actual SAR data, and specific metrics for SAR are evaluated. However, even the most elaborated speckle models are far from accounting for the complex mechanisms related to SAR images. In this paper, a methodology to design a realistic dataset to overcome these limitations is proposed. Actual SAR images of the same scene but acquired with the same sensor on different dates are downloaded from one of the available satellite platforms. Images are properly co-registered and averaged to get a ground truth-like reference image to objectively evaluate the performance of a despeckling method. To show the benefits of the proposed methodology, an on-the-shelf deep learning approach is used to filter the data, and compared with the standard approach using synthetic corrupted images with a speckle model. The final validation on actual SAR data not included in the training phase validates the proposed dataset. From the results shown, it is recommended to test filters on the proposed more realistic dataset and abandon the usual approach.**

***Index Terms*—Synthetic Aperture Radar (SAR), speckle noise, autoencoder (AE), supervised learning, multitemporal fusion**

I. INTRODUCTION

SAR (Synthetic Aperture Radar) images are corrupted by speckle which is caused by the use of coherent illumination and the complex backscatter mechanisms involved in the return radar signal, so no ground truth is available, which is a problem for assessing the performance of any filter [1]. To overcome this, in the seminal work by Lee et al. [2], a protocol is proposed: optical (natural) images are considered as noiseless data and then, using a suitable speckle model (i.e. Gamma distribution law) are properly corrupted, therefore, both, the noiseless and the speckled image are available and evaluated through well-established objective metrics and also visually by an expert. Moschetti et al. [3] replaced the one single synthetic image used in Lee's protocol, with massive Monte Carlo runs, providing more statistical significance to results. In other works, the speckle is physically simulated [4]. After being tuned on synthetic/modeled data, despeckling filters are then evaluated on actual SAR data.

A radically different approach has emerged recently ([5], [6], [7]) in which a more realistic SAR dataset for training is obtained from multitemporal average of SAR images in order to get a more realistic reference image. The effect of averaging the images provides a result somehow equivalent to the one from the common multi look technique. Then, such *ground truth* is corrupted with a speckle model with different levels of noise. In doing so, the limitations of the speckle model are notably reduced. The benefits and the drawback related to training deep learning networks on both, synthetic data and on the temporal multi looking approach are addressed in [8].

Our approach resembles to [5] in the sense of employing a multitemporal average of SAR data. However, in our case, the dataset is then used as it is, both for training and also in the evaluation of filter performances (in our last model the *ground truth* images are not corrupted with simulated speckle). A comparison with the common approach that relies on using corrupted data by a speckle model invites us to replace such a long-term way of working with the new methodology. This new methodology, although addressed in [8], where is said, sic. *"On the contrary, the approach based on simulation is quite risky if the simulated data are not really aligned with the test data"*, has not been soundly proposed as a new approach to replacing the old ones based on Lee's protocol. Note that we proposed this new methodology not only for assessing deep learning-based despeckling filters but for all despeckling filters.

This paper is organized as follows, in Section II we introduce the SAR speckle model and also review different approaches, traditional (local and non-local) and even DL-based despeckling filters. The new protocol is summarized in Section III. In Section IV the proposed framework to design a labeled dataset that includes ground truth and noisy images is explained. In Section V a default autoencoder (AE) is trained by using the designed dataset in order to demonstrate the convergence and the good performance of the model. Finally in Section VI some conclusions and future work are shown.

II. SPECKLE MODEL

The speckle is considered a multiplicative noise. A SAR image Y can be expressed as $Y = f(X, N) = X \cdot N$, where X is the noise-free image and N is the speckle noise, which has a Gamma distribution Eq. 1:

Manuscript received June 7th, 2023; accepted June XXth, 2023. Date of publication June XXth, 2023; date of current version June 7th, 2023.

[1]Rubén Darío Vásquez-Salazar is with the Faculty of Engineering, Politécnico Colombiano Jaime Isaza Cadavid, Medellín, Colombia, 48th Av, 7-151 (e-mail: rdvasquez@elpoli.edu.co)

[2]Ahmed Alejandro Cardona-Mesa is with the Faculty of Engineering, Institución Universitaria Digital de Antioquia, Medellín, Colombia, 55th Av, 42-90 (e-mail: amhed.cardona@iudigital.edu.co)

[3]Luis Gómez is with the Signal and Communications Department and Electronic Engineering Department, Universidad de Las Palmas de Gran Canaria, Las Palmas de Gran Canaria, Spain, Juan de Quesada 30 (e-mail: luis.gomez@ulpgc.es)

[4]Carlos M. Travieso-Gonzalez is with the Signals and Communications Department, IDeTIC, Universidad de Las Palmas de Gran Canaria, Spain. (e-mail: carlos.travieso@ulpgc.es)

$$p(N) = \frac{1}{\Gamma(L)} N^L e^{-NL}, \quad (1)$$

where L is the Equivalent Number of Looks (ENL) of the SAR image. As an active area of research in the last decades, the irruption of the deep learning (DL) paradigm has established a clear division of all methods: traditional despeckling filters and DL-based ones.

A. Speckle filtering

Different approaches for despeckling filters have been presented. Local filters like Lee and Redefined Lee filter [9], Frost and its proposed variants [10], among others. Non-local filters, which replace the value of a pixel with the average of similar pixels that have no reason to be close at all [11], non-local based on anisotropic diffusion (SRAD) which exploits the instantaneous coefficient of variation [12], a Nonlocal SAR Image Denoising Algorithm Based on LLMMSE Wavelet Shrinkage (SAR-BM3D) [13] and its improvement to make SAR-BM3D faster but keeping similar and good performance (FANS) [14].

B. DL in SAR despeckling

Different techniques that use DL have been also proposed. Some of the most relevant described in the review are: Generative Adversarial Networks (GAN) [15], SAR-CNN [16], DNN [17] and SAR-RDCP [18].

Neigh CNN [19] is a SAR speckle reduction proposal that uses a feature preserving loss function that includes: the Euclidean, the perpetual, and the neighborhood loss, obtaining better results compared to Kuan, SAR-BM3D, SARDRN, and IDCNN. Another proposal with a modified cost function, including the Kullback–Leibler divergence, is called Multi-Objective CNN-Based (MONET) [5], has shown improved SSIM, SNR, and MSE despeckling over non-local filters like NOLAND, ID-CNN, SAR-DRN, SAR-BM3D, and FANS. The cost function that will be used at the end of this paper is Binary Cross-Entropy / Log Loss, according to Eq. 2.

$$H_p(q) = -\frac{1}{N} \sum_{i=1}^{N} y_i \cdot log(p(y_i)) + (1-y_i) \cdot log(1-p(y_i)). \quad (2)$$

III. The New Protocol

The new protocol proposed in this work has been designed for assessing SAR filter despeckling of actual SAR data through either standard filters or DL filters. For a noisy image Y and its filtered version, F, the new protocol is simple and it consists of the following steps:

- Select a set of well-known SAR specific metrics, such as preservation of radiometric statistical properties measured on the ratio image (pixelwise division of Y and F: Y/F), the ENL (Equivalent Number of Looks), the mean preservation and noise variance reduction after filtering. Such metrics do not require a ground truth.
- Select a set of well-known referenced image quality indices to evaluate edges/small features/bright scatterers preservation and statistical structure of filtered data. These metrics require a ground truth to compare with. If not available, build a realistic SAR ground truth data set (see Section IV).
- Do not evaluate on a single filtered result but on as many despeckled outcomes as possible. If not possible, the evaluation must be done on several selected patches within the filtered results.
- Complement the numerical evaluation of filtered and ratio images with a visual inspection by an expert .
- Complement the evaluation (numerical and visual) with a comparison with state-of-the art despeckling filters.

This new protocol differs from the standard one in two radical things: first, it does not use a synthetic pattern. Secondly, it promotes the use of both, referenced metrics and of referenceless metrics

This new protocol may be used to evaluate the performances of a new proposed filter although it is also recommended for tuning a new filter. The design of the filter should be done on actual SAR data and not on synthetic SAR data. In the rest of the paper, the benefits of this new protocol are illustrated for the case of a DL filter and for a well-known state-of-the art filter.

IV. The Dataset

Actual SAR imagery is not easily accessible and available to any user. In [13] and [5] classical optical noise-free images are used which are initially and their speckled version is obtained through a distribution like the discussed Gamma to test the performance of despeckling filters. An analysis of three different approaches for building datasets is performed in [20].

A. Actual SAR imagery download

In this paper, we use ASF Datasearch Vertex [21]. Sentinel-1A imagery is available for download and we chose a region with urban areas and man-made structures like bridges, buildings, highways, and so on. The images correspond to the region of Toronto in 2022. For the purpose of this paper, images in intensity mode level *"L1 Detected High-Res Dual-Pol (GRD-HD)"* of the same location acquired from Aug 24th to Dec 22nd with a revisiting period of 12 days, were downloaded. The images were obtained with the C band at 5.4GHz with a resolution of 20m, VV polarization at a height of 693km from Ecuador. Some of their technical specifications are described in Table I.

TABLE I
Technical specifications of downloaded SAR images

ITEM	DESCRIPTION
Mission	Sentinel 1A
Band	C (5.4GHz)
Beam mode	IW
Resolution	20m
Flight direction	Ascending
Polarization	VV
Height at Ecuador	693km

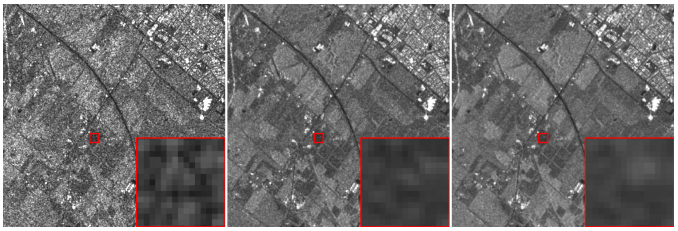

Fig. 1. Actual SAR image and averages 5 and 10 respectively (from left to right) with a zoom of a 20x20 window in red rectangles of a homogeneous area

B. Multitemporal fusion

Multitemporal fusion (or temporal multi-looking) is a mean operation performed over several images of the same location. In our case, a reference image of September 5th is selected, other four and then other nine images are registered and averaged with respect to it, as shown in Fig. 1. The ENL of the three images is calculated in two large enough regions of interest of 20×20 pixels selected in a homogeneous area (red squares). The corresponding ENLs of the images in the bottom of the regions of interest of the figure are (from left to right): 16.490, 50.015, and 70.605 respectively. As expected, including more images in the mean operation results in a less noisy image (higher ENL). A mean of 10 samples will be used in this paper.

C. Image clipping

This process can be performed through three main parameters: the desired width of the clipped images (W), the desired height of the clipped images (H), and the stride (S). A recommended setting that we make of these parameters is $W = H = S = 512$. With this setting, from the downloaded image of 26019×16732 pixels, it is possible to obtain 1600 clipped images of 512×512 pixels. A smaller stride will generate more images but some of the pixels will be overlapped between images, which could be considered a data augmentation technique what is a common practice in artificial intelligence and DL. The size of the image must be a power of 2, because of the dimension-reducing steps in DL, such as MaxPooling with a stride of 2. The code used in the previous sections is available at https://github.com/rubenchov/SAR_despeckling_dataset.

V. Experimental results

The experiments carried out in this paper include the training of two DL models. The *"SAR model"* was trained by using the designed dataset in IV. Another one, the *"Synthetic model"*, was built by using images corrupted according to Eq. (1) with $ENL = 16$, similar to the ENL measured in the actual SAR images. We also performed a despeckling process by applying the FANS filter to both datasets, since it is one of the state-of-the-art filters that do not include artificial intelligence, and thus it is a traditional reference filter in so many publications.

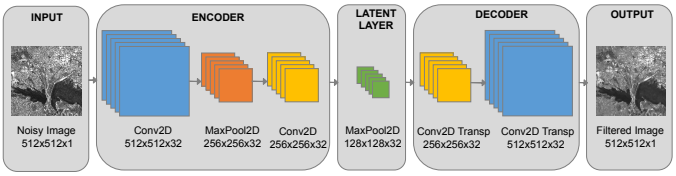

Fig. 2. Structure of the autoencoder composed of input, encoder, latent layer (bottleneck), decoder, and output

A. Structure of the Autoencoder

The structure of the DL models, in this case autoencoders (AE), was adapted from [22], by modifying its input and output dimensions, corresponding to the size of the designed dataset (512×512). The AE is composed of five main parts as shown in Fig. 2. The input is the noisy image, which in this case is a clip of 512×512 pixels. The image must be in grayscale, so the full size of the input is 512×512×1. The encoder is a layer of 32 convolutional 2D filters with RELU activation followed by a downsampling MaxPooling operation along its spatial dimensions (height and width) by taking the maximum value over an input window of size 2×2. Again another layer of 32 filters of 2D filters followed by a MaxPooling operation of size 2×2. The Latent layer, or bottleneck, has the image transformed with the smallest dimensions (128×128), one-fourth of the input size. This small dimension restricts the noise and only leaves the important information of the image, so, the autoencoder acts as a speckle filter. The Decoder is composed of two layers of transposed convolution, also called *"deconvolution"* of 32 filters. Finally, one layer consists of one last 2D convolution filter of size 3×3. Finally, the Output is a layer that delivers a new grayscale image, resulting from the compression and decompression of the autoencoder, a process in which the noise was reduced. The output has the same size (512×512×1) that the input of the AE.

B. Training process

The optimizer is trained by using an Adam optimizer and the Binary Cross Entropy (BCE) loss function according to Eq. 2. The designed dataset is composed of 3200 images (1600 noisy and 1600 ground truth) but 6 images were removed from this dataset to build a separate validation set. Once the model is trained, when a new noisy image is fed, the output will be a filtered image.

C. Metrics for SAR despeckling

The evaluation of despeckling filters can be divided into two categories. The first one (known as referenced assessing), requires a ground truth. The second one is known as reference-less assessing and is the one generally used for actual SAR data.

Among the metrics that require a ground truth, the most used are the Mean Squared Error (MSE), the Peak Signal Noise Ratio (PSNR), and Structural Similarity Index Measure (SSIM). For actual SAR data (no ground truth available), the most used is the ENL. The $\mathcal{M}$ estimator proposed in

[23] is a referenceless metric that operates within the ratio image (the pixel-wise division of the original image and the filtered image) and it measures both, the preservation of the radiometric properties of the ratio image and its statistical properties. A perfect despeckling filter will produce $\mathcal{M} = 0$ (the ratio image resembles pure speckle).

D. Despeckling results

Some of the results of training two DL models and applying the FANS filter over the two datasets, including ratio images used to calculate the $\mathcal{M}$-estimator, are shown in Fig. 3, namely samples 1 (column 1), 2 (column 2), and 3 (column 3). Five different metrics and indexes (ENL, PSNR, MSE, SSIM, and $\mathcal{M}$) were applied to validate the results, as shown in Table. II, the best outcomes for each sample with every type of noise are highlighted with bold formatting across all performance metrics. The FANS filter performed best than the AE in the synthetic type of noise, even though the results of the AE were very close, especially in PSNR and SSIM. The AE performed best in the actual SAR images in all cases for the metrics ENL, PSNR, MSE, and SSIM. $\mathcal{M}$ was lower with FANS over synthetic noise only in one of the three samples with respect to the AE.

TABLE II
ENL, PSNR, MSE, SSIM AND $\mathcal{M}$-ESTIMATOR OF 3 VALIDATION SAMPLES DESPECKLED AND EVALUATED WITH TWO DIFFERENT FILTERS

VALIDATION SAMPLE	TYPE OF NOISE	IMAGE	ENL	PSNR	MSE	SSIM	M
1	No noise	Ground Truth	85.358	-	-	-	-
	Synthetic	Noisy	13.673	17.557	1141.199	0.379	-
		Filtered FANS	**422.418**	**25.033**	**204.032**	**0.710**	26.666
		Filtered AE	157.625	24.739	218.360	0.709	**20.496**
	SAR	Noisy	17.614	18.418	936.101	0.526	-
		Filtered FANS	104.488	21.156	498.319	0.649	**55.035**
		Filtered AE	**153.375**	**22.672**	**351.425**	**0.667**	78.246
2	No noise	Ground Truth	200.631	-	-	-	-
	Synthetic	Noisy	13.495	18.386	943.020	0.431	-
		Filtered FANS	**398.504**	**25.694**	**175.241**	**0.775**	**11.366**
		Filtered AE	243.027	25.062	202.734	0.758	19.349
	SAR	Noisy	18.066	18.886	840.318	0.558	-
		Filtered FANS	105.902	21.217	491.321	0.692	**39.560**
		Filtered AE	**629.345**	**22.615**	**356.139**	**0.707**	65.429
3	No noise	Ground Truth	189.796	-	-	-	-
	Synthetic	Noisy	14.513	19.184	784.623	0.396	-
		Filtered FANS	**980.917**	**25.932**	**165.923**	**0.803**	**33.167**
		Filtered AE	314.039	25.531	181.950	0.792	35.841
	SAR	Noisy	17.374	19.599	713.116	0.537	-
		Filtered FANS	108.848	21.576	452.377	0.721	**107.560**
		Filtered AE	**459.234**	**22.881**	**334.965**	**0.764**	124.961

To validate the effectiveness of the traditional Lee's protocol, three additional samples (namely 4, 5, and 6) were selected from the Land-Use Scene Classification dataset [24]. These optical images were corrupted with synthetic speckle noise, where the ENL was set to 16. The denoising outcomes obtained using the FANS method are shown in Fig. 4.

The results of Table III in boldface demonstrate a significant improvement achieved by the FANS filter in the optical case, compared to those obtained in Table II. It is evident that the FANS filter outperforms all cases involving synthetic noise. These findings indicate that the FANS filter is well-suited for synthetic models; however, it falls short in accurately modeling and denoising the speckle in actual SAR images. The AE trained with the *"SAR dataset"* learned from them actual SAR images, including the speckle, and effectively removed it. As a result, the AE significantly improves the metrics of ENL, PSNR, MSE, and SSIM over actual SAR images, as was shown in Table II.

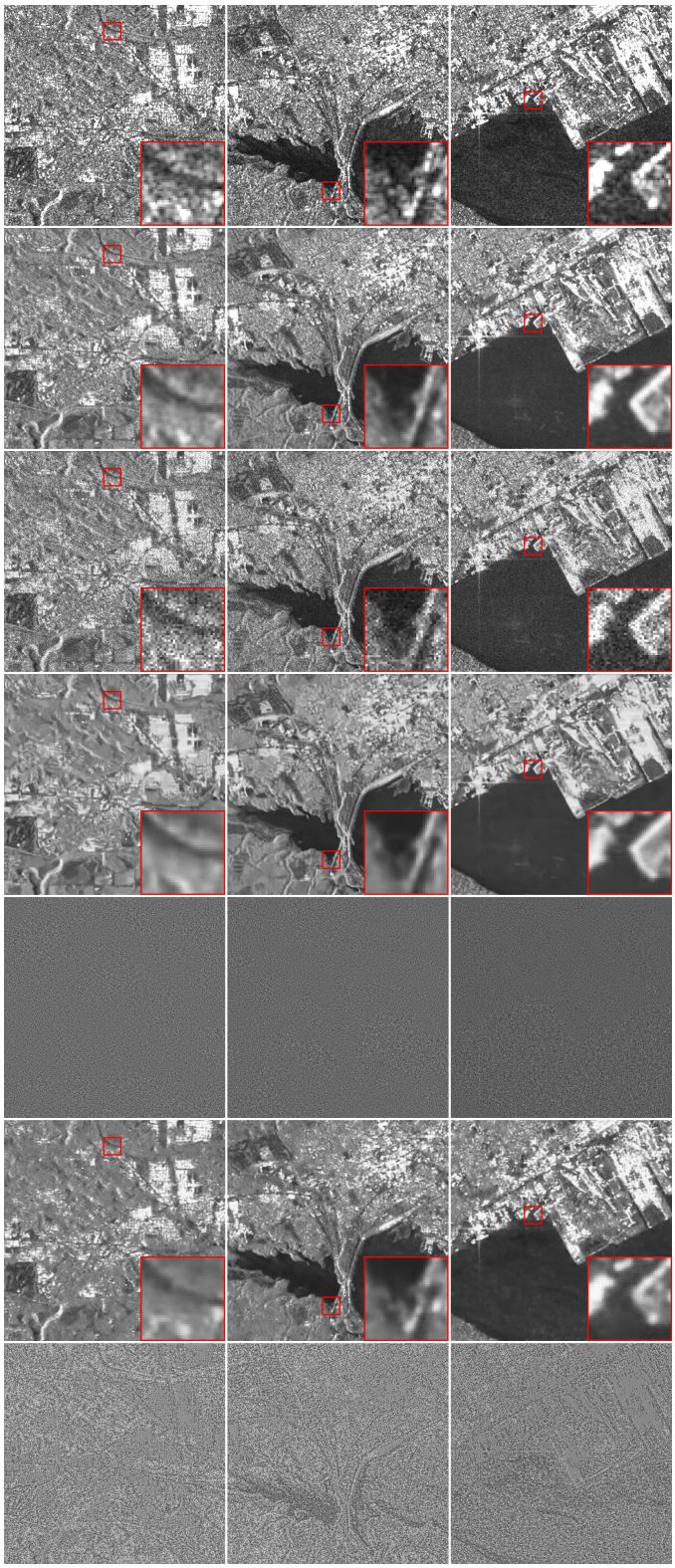

Fig. 3. Comparison of validation images (top to bottom): Actual SAR, generated ground truth, ground truth corrupted with synthetic noise ENL=16, synthetic denoised with FANS and ratio images, SAR denoised by AE trained with actual SAR images and ratio images

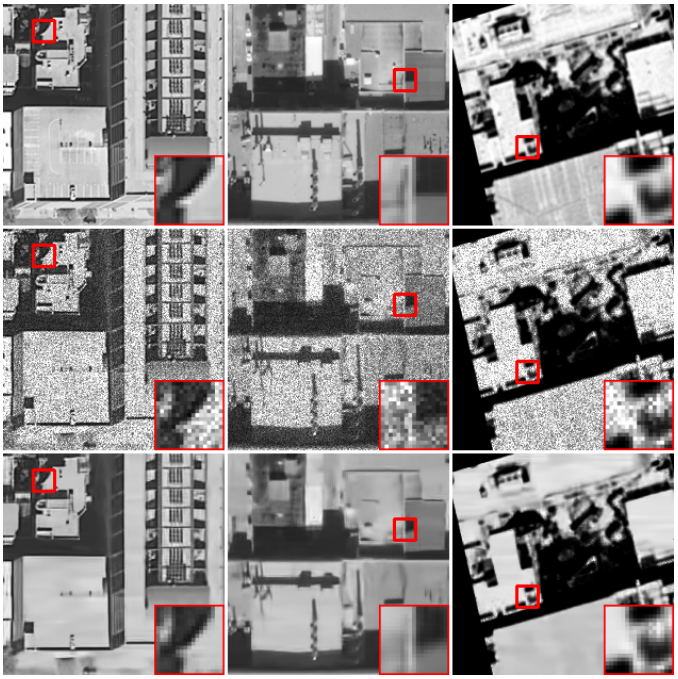

Fig. 4. Comparison of optical images from Kaggle. (Top) Optical (no noise). (Middle) Corrupted with synthetic noise ENL=16. (Bottom) Denoised by FANS with the same ENL=16

TABLE III
ENL, PSNR, MSE, SSIM AND $\mathcal{M}$-ESTIMATOR OF THREE OPTICAL IMAGES DENOISED WITH FANS FILTER ACCORDING TO LEE'S PROTOCOL

VALIDATION SAMPLE	TYPE OF NOISE	IMAGE	ENL	PSNR	MSE	SSIM	M
4	No noise	Ground Truth	3735.34	-	-	-	-
	Synthetic	Noisy	21.60	17.34	1196.49	0.47	-
		Filtered FANS	**1886.04**	25.67	176.34	**0.83**	24.19
5	No noise	Ground Truth	1463.08	-	-	-	-
	Synthetic	Noisy	22.92	17.88	1060.56	0.361	-
		Filtered FANS	**9752.33**	**28.44**	**92.89**	**0.85**	18.24
6	No noise	Ground Truth	2081.79	-	-	-	-
	Synthetic	Noisy	19.93	17.91	1052.98	0.57	-
		Filtered FANS	**3625.23**	25.55	180.61	**0.83**	**1.21**

VI. CONCLUSION AND FUTURE WORK

The labeled *"SAR dataset"* was designed by creating two folders, one with noisy and another with ground truth images. An autoencoder with default parameters was trained and its results were analyzed, finding that the metrics evaluated (ENL, PSNR, MSE, SSIM, and ENL) were significantly improved over SAR images compared to a filter by using the traditional synthetic approach.

In general, the best performance over SAR images was obtained from the *"SAR model"*, so we recommend stopping the use of the synthetic approach and starting the use of actual SAR images for all the filter validations whenever the multitemporal images are available.

This framework shows promising results and opens an enormous possibility for more researchers to design and evaluate their own labeled dataset to train DL-based models for image despeckling and obtain much better results in SAR applications.

REFERENCES

[1] Fabrizio Argenti, Alessandro Lapini, Tiziano Bianchi, and Luciano Alparone. A tutorial on speckle reduction in synthetic aperture radar images. *IEEE Geoscience and Remote Sensing Magazine*, 1(3):6–35, 2013.

[2] J. S. Lee, L. Jurkevich, P. Dewaele, P. Wambacq, and A. Oosterlinck. Speckle filtering of synthetic aperture radar images: A review. *Remote Sensing Reviews*, 8(4):313–340, 1994.

[3] E. Moschetti, M. G. Palacio, M. Picco, O. H. Bustos, and A. C. Frery. On the use of Lee's protocol for speckle-reducing techniques. *Latin American Applied Research*, 36:115–121, 2006.

[4] Gerardo Di Martino, Antonio Iodice, Daniele Riccio, and Giuseppe Ruello. Physical models for SAR speckle simulation. In *2012 IEEE International Geoscience and Remote Sensing Symposium*, pages 5782–5785, 2012.

[5] Sergio Vitale, Giampaolo Ferraioli, and Vito Pascazio. Multi-objective cnn-based algorithm for SAR despeckling. *IEEE Transactions on Geoscience and Remote Sensing*, 59:9336–9349, 2020.

[6] D. Cozzolino, L. Verdoliva, G. Scarpa, and G. Poggi. Nonlocal SAR image despeckling by convolutional neural networks. In *IGARSS 2019 - 2019 IEEE International Geoscience and Remote Sensing Symposium*, pages 5117–5120, 2019.

[7] G. Chierchia, D. Cozzolino, G. Poggi, and L. Verdoliva. SAR image despeckling through convolutional neural networks. In *2017 IEEE International Geoscience and Remote Sensing Symposium (IGARSS)*, pages 5438–5441, 2017.

[8] A. Mazza, G. Scarpa, L. Verdoliva, and G. Poggi. Impact of training set design in cnn-based SAR image despeckling. In *2021 IEEE International Geoscience and Remote Sensing Symposium IGARSS*, pages 415–418, 2021.

[9] Aiyeola Sikiru Yommy, Rongke Liu, and Shuang Wu. SAR image despeckling using refined Lee filter. In *2015 7th International Conference on Intelligent Human-Machine Systems and Cybernetics*, volume 2, pages 260–265, 2015.

[10] Sriparna Banerjee, Sheli Sinha Chaudhuri, Raghav Mehra, and Arundhati Misra. A comprehensive survey on frost filter and its proposed variants. In *2020 5th International Conference on Communication and Electronics Systems (ICCES)*, pages 109–114, 2020.

[11] Antoni Buades, Bartomeu Coll, and Jean-Michel Morel. Non-local means denoising. *Image Processing Online*, 1, 2011.

[12] Yongjian Yu and Scott T. Acton. Speckle reducing anisotropic diffusion. *IEEE Transactions on Image Processing : a publication of the IEEE Signal Processing Society*, 11 11:1260–70, 2002.

[13] Sara Parrilli, Mariana Poderico, Cesario Vincenzo Angelino, and Luisa Verdoliva. A nonlocal SAR image denoising algorithm based on llmmse wavelet shrinkage. *IEEE Transactions on Geoscience and Remote Sensing*, 50:606–616, 2012.

[14] Davide Cozzolino, Sara Parrilli, Giuseppe Scarpa, Giovanni Poggi, and Luisa Verdoliva. Fast adaptive nonlocal SAR despeckling. *IEEE Geoscience and Remote Sensing Letters*, 11:524–528, 2014.

[15] Ian J. Goodfellow, Jean Pouget-Abadie, Mehdi Mirza, Bing Xu, David Warde-Farley, Sherjil Ozair, Aaron C. Courville, and Yoshua Bengio. Generative adversarial nets. In *NIPS*, 2014.

[16] Giovanni Chierchia, Davide Cozzolino, Giovanni Poggi, and Luisa Verdoliva. SAR image despeckling through convolutional neural networks. In *2017 IEEE International Geoscience and Remote Sensing Symposium (IGARSS)*, pages 5438–5441. IEEE, 2017.

[17] Dong-Xiao Yue, Feng Xu, and Yaqiu Jin. SAR despeckling neural network with logarithmic convolutional product model. *International Journal of Remote Sensing*, 39:7483 – 7505, 2018.

[18] Huanfeng Shen, Chen Zhou, Jie Li, and Qiangqiang Yuan. SAR image despeckling employing a recursive deep cnn prior. *IEEE Trans. Geosci. Remote. Sens.*, 59:273–286, 2021.

[19] Praveen Ravirathinam, Darshan R Agrawal, and J. Jennifer Ranjani. Neighcnn: A cnn based SAR speckle reduction using feature preserving loss function. *ArXiv*, abs/2108.11573, 2021.

[20] Sergio Vitale, Giampaolo Ferraioli, and Vito Pascazio. Analysis on the building of training dataset for deep learning SAR despeckling. *IEEE Geoscience and Remote Sensing Letters*, 19:1–5, 2022.

[21] NASA. ASF data search, 2023. Accessed on March 24, 2023.

[22] Santiago L Valderrama. Keras documentation: Convolutional autoencoder for image denoising. https://keras.io/examples/vision/autoencoder/, Mar 2021. [Online; accessed 29-May-2023].

[23] Luís Gómez Déniz, Raydonal Ospina, and Alejandro César Frery. Unassisted quantitative evaluation of despeckling filters. *Remote. Sens.*, 9:389, 2017.

[24] Dahiya Gotam. Land-use scene classification. https://www.kaggle.com/datasets/apollo2506/landuse-scene-classification, 2020. [Online; accessed 29-May-2023].